

KEK 83-11
July 1983
TRISTAN(E)

QUENCH SIMULATION IN THE THIN SUPERCONDUCTING SOLENOID

T. TOMINAKA, M. TAKASAKI, M. WAKE and R. YAMADA

NATIONAL LABORATORY FOR
HIGH ENERGY PHYSICS

© National Laboratory for High Energy Physics, 1983

KEK Reports are available from:

Technical Information Office
National Laboratory for High Energy Physics
Oho-machi, Tsukuba-gun
Ibaraki-ken, 305
JAPAN

Phone: 0298-64-1171
Telex: 3652-534 (Domestic)
(0)3652-534 (International)
Cable: KEKOH0

Quench Simulation in the Thin Superconducting Solenoid

T. Tominaka[†], M. Takasaki, M. Wake and R. Yamada*

National Laboratory for High Energy Physics, KEK

Oho-machi, Tsukuba-gun, Ibaraki-ken, 305 Japan

*Fermi National Accelerator Laboratory, Batavia, Ill. USA

Abstract

The propagation velocities of a normal zone were calculated for a 1 mφ × 1 m superconducting solenoid and for a 3 mφ × 5 m thin solenoid based on a simple model using the one-dimensional thermal equation. The quench back effect can be observed in certain conditions. The quench of the large thin solenoid was also simulated by using the computer program 'QUENCH'.

KEYWORDS: quench, simulation, superconducting, magnet

[†]Postdoctoral Fellow of the Japan Society for the Promotion of Science

1. Introduction

To avoid the breakdown of a superconducting magnet during a quench, we estimate the quench characteristics of the magnet, i.e. the current decay, the coil voltage development, the coil temperature rise, etc. applying the computer program 'QUENCH'.¹ The results strongly depend on the quench velocity (or the propagation velocity of a normal zone). To obtain reliable estimation of quench characteristics of the solenoid, we calculated the quench velocities modifying a simple model². The quench back effect³ can be observed on the large thin solenoid even with an aluminum bobbin of high electrical resistance.

2. Quench Velocity in the Axial Direction

The model adopted for the spread of a normal zone in the axial direction of a solenoid is illustrated in Fig. 1. Using a computer program of the finite difference calculus, we solved the one-dimensional thermal conduction equation in MKS after a quench was started as follows;

$$\gamma C_p(T) \frac{\partial T}{\partial t} = \frac{\partial}{\partial y} (k_1 \frac{\partial T}{\partial y}) + Q_j(T) + \frac{d_b}{d_c + d_b} \frac{\mu_0^2 r_b^2 d_c^2}{4 \rho_b \tau^2} j^2. \quad (1)$$

$$\begin{aligned} Q_j(T) &= 0, & T < T_c. \\ &= \rho_c(T) j^2 (T - T_c) / (T_{c0} - T_c), & T_c \leq T \leq T_{c0}. \\ &= \rho_c(T) j^2, & T_{c0} < T. \end{aligned} \quad (2)$$

where

γ = Density of the conductor,

C_p = Heat capacity per unit mass of axially one-dimensional rod,

k_1 = Averaged thermal conductivity in the axial direction,

ρ_c = Electrical resistivity of the conductor,

d_c = Radial thickness of the conductor,
 d_b = Radial thickness of the bobbin,
 r_b = Radius of the bobbin,
 ρ_b = Electrical resistivity of the bobbin,
 τ = Effective decay time constant of the solenoid current,
 j = Averaged current density of solenoid current over the area of the conductor,
 μ_0 = Permeability,
 T_c = Current sharing temperature of the composite superconductor,
 T_{c0} = Critical temperature of the composite superconductor at zero current.

The last term of Eq. (1) represents the effect due to the eddy current loss in the bobbin (see Appendix A). This calculation is based on the following assumptions;

- (1) There is no heat flow along the conductor in the circumferential direction.
- (2) The averaged thermal conductivity k in the axial direction is estimated from the thermal conductivity of the conductor (Al) $k_{con} = \sim 10^3$ W/m \cdot K, the width of the conductor $l_{con} = 3.59$ mm, the thermal conductivity of insulator (Epoxy) $k_{ins} = \sim 7 \times 10^{-2}$ W/m \cdot K and the width of the insulator $l_{ins} = 0.1$ mm using

$$\frac{l_{tot}}{k_i} = \frac{l_{con}}{k_{con}} + \frac{l_{ins}}{k_{ins}}, \text{ where } l_{tot} = l_{con} + l_{ins}$$

Approximately,

$$k_i \approx \frac{l_{tot}}{l_{ins}} k_{ins}. \quad (3)$$

The averaged thermal conductivity k could be treated as a fitting parameter, to compare with the data of the quench velocities for the $1 \text{ m}\phi \times 1 \text{ m}$ solenoid.

- (3) The heat generated by the eddy current loss in the bobbin spreads homogeneously over both the bobbin and the conductor. The thermal contact between the bobbin and the conductor is good, and the time delay due to thermal conductivity between them is neglected.
- (4) The heat flow from the conductor to the bobbin is neglected, and the cooling effect of liquid helium is also neglected.

The electrical resistivity $\rho_c(T)$ of the conductor and the heat capacity $C_p(T)$ are approximated by the following equations,

$$\begin{aligned} \rho_c(T) &= A \cdot T^{AEX} & A, AEX: \text{parameters} \\ C_p(T) &= C \cdot T^{CEX} & C, CEX: \text{parameters} \end{aligned}$$

for the temperature ranges considered⁴. The thermal conductivity $k = 2.6$ W/m \cdot K and the electrical resistivity $\rho_b = 3.05 \times 10^{-8}$ Ωm of the bobbin are assumed to be constant over the temperature ranges considered. The eddy current loss of the conductor and banding are also neglected.

3. Calculated Results of the Temperature Distribution and the Quench Velocity

The time evolution of the temperature distribution and the quench velocity were calculated for the $1 \text{ m}\phi \times 1 \text{ m}$ solenoid and for a $3 \text{ m}\phi \times 5 \text{ m}$ thin solenoid.

1 mφ × 1 m Solenoid

A typical plot of the time dependence of the temperature distribution and the position dependence of the calculated quench velocities are shown in Figs. 2 and 3. In Fig. 3, the quench velocity is observed to become faster in the course of time especially at higher solenoid current. The experimental and calculated results of quench velocities are compared in Fig. 4^{5,6}. The calculated results roughly agree with experimental ones with the fitted value of $k = 1.6 \text{ W/m}\cdot\text{K}$. This discrepancy may be due to the assumptions or the value of $\rho_c(T)$. The effect of the eddy current loss in the 1 mφ × 1 m coil is not large enough to make a 'quench back'.

3 mφ × 5 m Solenoid

The simulated results of the 3 mφ × 5 m solenoid are shown in Figs. 5 and 6. It reveals that at the beginning the quench velocity increases gradually with the elapse of time or with the distance from the initial normal zone. After some duration of time, the minimum temperature of the coil goes up to the critical temperature. Until 0.46 sec after the start of the quench, the conductor gets warmer due to the eddy current heating of the bobbin, and the quench velocity becomes faster. At 0.46 sec, the temperature of the whole conductor exceeds the critical temperature. All of a sudden, the whole conductor goes to normal.

This shows that the simple computer program can predict the phenomenon of a 'quench back' in the 3 mφ × 5 m solenoid, which was not observed in the 1 mφ × 1 m solenoid. The resulting resistive voltage in the coil after the quench back is distributed over the whole coil and is counteracted by the distributed inductive voltage, therefore the net maximum voltage will be small.

4. Simulation by the Computer Program 'QUENCH'

The computer program QUENCH was originally developed at Rutherford and has been applied for the design of the 1 mφ × 1 m coil and the 3 mφ × 5 m solenoid. Once again this QUENCH program was applied to the 3 mφ × 5 m solenoid under various conditions such as different time constants and the different quench origins.

Our version of the program QUENCH was obtained from forth CDC-CYBER at Fermilab and converted for the HITAC-M200H. Some improvements such as the capability of graphic output were made in addition to the conversion.

In this program the quench velocity U along the conductor (or in the circumferential direction of solenoid) is given by the initial propagation velocity U_0 (cm/sec) as follows,⁷

$$U = U_0 \frac{I}{I_0},$$

where I and I_0 are the present and the initial current. U_0 is given by

$$U_0 = \frac{j_0}{\gamma C_p} \sqrt{\frac{\rho k}{T_c - T_0}} = \frac{I_0}{A \gamma C_p} \sqrt{\frac{\rho k}{T_c - T_0}} = \frac{I_0}{A \gamma C_p} \sqrt{\frac{L I_c^2}{T_c - T_0}} \quad (4)$$

where

j_0 = Initial current density of the conductor (A/cm^2),

A = Cross sectional area of the conductor (cm^2),

γ = Averaged density of the conductor (g/cm^3),

C_p = Averaged specific heat of the conductor (J/g),

ρ = Electrical resistivity of the stabilizer (Ωcm),

k = thermal conductivity of the stabilizer ($\text{W}/\text{cm}\cdot\text{K}$),

T_c = Transition temperature (K),

T_0 = Operating temperature (K),

$L =$ Lorentz number $(= 2.45 \times 10^{-8} \text{ W}\Omega/\text{K}^2)$.

The transition temperature T_c is approximated by the mean between the current sharing temperature T_{c0} ($= 6.4 \text{ K}$ at 1.5 T and 4500 A) and the critical temperature at zero current T_{c0} ($= 8.6 \text{ K}$ at 1.5 T). The volumetric specific heat γC_p is taken at T_c . From the Wiedemann-Franz Lorentz law, the averaged value of ρk is written $\rho k = LT_c$. In the program 'QUENCH' the last equation of Eq. (4) was used.

The transverse quench velocity U_c in the axial direction is given by

$$\begin{aligned} U_c &= \epsilon U, \\ \epsilon &= \sqrt{k_L/k}, \end{aligned} \quad (5)$$

where k is the averaged thermal conductivity in the perpendicular direction and k that in the conductor direction.

The input data of electrical resistivity of aluminum and copper, and those of heat capacity of aluminum, copper, titanium and niobium for the program 'QUENCH' are plotted as a function of temperature in Figs. 7 and 8 respectively. However, the electrical conductivity of NbTi in the normal state is neglected.

1 mφ × 1 m Solenoid

For the 1 mφ × 1 m solenoid (conductor size $2.0 \times 0.359 \text{ cm}^2$), the transverse quench velocity (in the axial direction) derived from Eq. (5) is also plotted in Fig. 4. This adiabatic transverse quench velocities are much larger than experimental ones. This difference many originate from neglect of the cooling effect by adjacent parts and liquid helium, the inaccurate estimation of transition temperature, etc. The estimation of current density in Eq. (4) may also not be adequate, because, after the transition to normal conductivity, the diffusion time of

current distribution across the aluminum matrix is not small.⁸

3 mφ × 5 m Solenoid

We tried to estimate the quench characteristics of the full-size solenoid by the above-mentioned method. With the condition of the magnet current 4500 A (or overall current density $= 4.2 \times 10^7 \text{ A/m}^2$), the calculated results are summarized in Table 1 - 4. In Table 1, the quench characteristics for the cases with various external dump (or protection) resistors are summarized. The longitudinal quench velocity is 0.18 m/sec. Since the diameter of the solenoid is 3.0 m, this transverse quench velocity means the effective longitudinal velocity of 140 m/sec. For the case with a dump resistor of 50 mΩ, the time variation of the magnet current, the coil resistance, the resistive coil voltage and the maximum coil temperature are shown in Fig. 9. The case when the power supply does not turn off by an accident corresponds to M-1 of Table 1. In that case the resistance of 5 mΩ can be regarded as the resistance of power leads. Even in this case the solenoid seems to be safe.

From the Table 1, it can be seen that the maximum temperature rise after a quench T_{max} , is roughly related to the actual time constant of current decay (or current decay time) t_{act} though the following equation,⁷

$$\int_{T_0}^{T_{max}} \frac{\gamma C_p(T) dT}{\rho(T)} = \int_0^{\infty} J^2 dt \approx J_0^2 t_{act} \quad (6)$$

where γ = density, $C_p(T)$ = specific heat, $\rho(T)$ = resistivity and J = current density. Also the maximum resistive coil voltage V_{max} (resistive) is closely related to the maximum coil temperature by coil resistance.

In Table 2, the quench characteristics in the cases that the quench occurs from the edge of the coil are summarized. In comparison with the case that the quench occurs from the middle of the coil (Table 1), the propagation velocity of the normal zone in the coil becomes effectively smaller, and as a result the current decay time becomes larger. This is because the normal zone propagates in only one direction and the resulting internal resistance builds up slower than in the other case.

In Table 3, the quench characteristics for the arbitrarily chosen fast velocities corresponding to a 'quench back' are summarized. In comparison with the case of $R = 50 \text{ m}\Omega$ in Table 1, the current decay time becomes smaller, as a result of the large propagation velocity of the normal zone. The effect of the heat capacity of the bobbin can be taken for the quench calculation and is summarized in Table 4. The quench characteristics in this case are calculated by using effectively larger heat capacity of the conductor. Since the heat capacity in Eq. (6) becomes large, the current decay time becomes larger.

5. Conclusion

Quench propagation phenomena in thin superconducting solenoid magnets with aluminum stabilized conductors can be understood by solving the thermal equation in the conductors. The analysis which is consistent with the test result of the $1 \text{ m}\phi \times 1 \text{ m}$ solenoid predicts the quench back effect for the $3 \text{ m}\phi \times 5 \text{ m}$ magnet due to the eddy current in the bobbin of the solenoid. This effect will help the magnet to distribute the stored energy dissipation in the whole body of the magnet. A series of calculations using the program 'QUENCH' was carried out without the above quench back effect. Again, the analysis based on the $1 \text{ m}\phi \times 1 \text{ m}$

coil test data showed a substantial safety margin for the operation of the $3 \text{ m}\phi \times 5 \text{ m}$ solenoid.

Appendix A

Eddy Current Loss in the Bobbin During Quench

We consider the eddy current loss in the bobbin (A15083-0) with mean radius r , thickness d_b , length l , and resistivity $\rho = 3.05 \times 10^{-8} \Omega\text{m}$ in MKS. When the applied magnetic field $B(t)$ decays after a quench, the induced voltage $V(t)$, current $I(t)$, and the total power $P(t)$ are calculated as follows,

$$V(t) = \dot{\phi} = \pi r^2 \dot{B}(t),$$

$$I(t) = \frac{V}{R} = \frac{\pi r^2 \dot{B}(t)}{\frac{2\pi r}{\rho d_b l}} = \frac{r d_b l \dot{B}(t)}{2\rho},$$

$$P(t) = I(t)V(t) = \frac{\pi r^3 d_b l}{2\rho} [\dot{B}(t)]^2.$$

If the time constant of decay of the magnetic field is τ , i.e. $B(t) =$

$$B_0 e^{-t/\tau},$$

$$P(t) = \frac{\pi r^3 d_b l}{2\rho \tau^2} [B(t)]^2, \quad (\text{A-1})$$

$$p(t) = \frac{P(t)}{2\pi r d_b l} = \frac{r^2}{4\rho \tau^2} [B(t)]^2, \quad (\text{A-2})$$

where $p(t)$ is the power loss per unit volume. If the current density of the solenoid with thickness d_c is $j(t) = j_0 e^{-t/\tau}$,

Table 1. List of quench characteristics under various protection resistances, in the cases that the quench occurs from the middle of coil. R = protection resistance, L = inductance, t_{act} = actual (resulted) current decay time, T_{max} = maximum temperature, $V_{max}(res.)$ = maximum resistive voltage, $V_{max}(total)$ = maximum inductive voltage, E_{int} = energy dissipated in the coil, E_{ext} = extracted energy, $\int r^2(t)dt$ = time integral of the squared magnet current which relates to T_{max} (see refs. 4) and 7)).

Run #	R	L/R	T_{act}	T_{max}	$V_{max}(res.)$	$V_{max}(total)$	E_{int}	E_{ext}	$\int r^2(t)dt$
M-1	0.005 Ω	586. s	32.6 s	107. K	487. V	500. V	27. MJ	2.3 MJ	4.68×10^8 A ² sec
M-2	0.02 Ω	147. s	33.7 s	97.5 K	347. V	395. V	21. MJ	8.8 MJ	4.40×10^8 A ² sec
M-3	0.05 Ω	58.6 s	33.7 s	78.3 K	154. V	270. V	11. MJ	19. MJ	3.76×10^8 A ² sec
M-4	0.1 Ω	29.3 s	25.6 s	54.7 K	51.7 V	450. V	3.2 MJ	26. MJ	2.63×10^8 A ² sec
M-5	0.5 Ω	5.9 s	5.9 s	26.7 K	4.3 V	2250. V	0.07 MJ	29. MJ	0.61×10^8 A ² sec
M-6	1. Ω	2.9 s	2.9 s	21.3 K	2.0 V	4500. V	0.02 MJ	29. MJ	0.31×10^8 A ² sec

- * Initial quench velocity in the circumferential direction $U_z(\text{calc.}) = 4.44$ m/sec,
 Initial quench velocity in the radial direction $U_x(\text{calc.}) = 4.44$ m/sec,
 Initial quench velocity in the axial direction $U_y(\text{calc.}) = 0.178$ m/sec.

$$B(t) = \mu_0 d_c j(t) = \mu_0 d_c j_0 e^{-t/\tau},$$

$$P(t) = \frac{\mu_0^2 r^3 d_c^2}{2\rho r^2} [j(t)]^2, \quad (\text{A-3})$$

$$P(t) = \frac{\mu_0^2 r^2 d_c^2}{4\rho r^2} [j(t)]^2 \quad \text{per unit volume.} \quad (\text{A-4})$$

For example,

1. The power of eddy current loss of 1 m ϕ x 1 m coil in the case of $B_0 = 1.5$ T, $\tau = 47$ mH/45 m $\Omega = 1.0$ sec, and $r = 0.5$ m from Eq. (A-2), is

$$P(0) = \frac{0.5^2 \times 1.5^2}{4 \times 3.05 \times 10^{-9} \times 1.0^2} = 4.6 \times 10^6 \text{ W/m}^2.$$

2. The power of CDF solenoid in the case of $B_0 = 1.5$ T, $\tau = 2.93$ H/50 m $\Omega = 58.6$ sec and $r = 1.5$ m, is

$$P(0) = \frac{1.5^2 \times 1.5^2}{4 \times 3.05 \times 10^{-9} \times 58.6^2} = 1.2 \times 10^4 \text{ W/m}^2.$$

References

1. M. N. Wilson, RHEL/M-151, Internal Report (1968).
2. H. Ogata, Engineering Sheet/CDF-0-6 (1982) [in Japanese].
3. M. A. Green, Cryogenics 17 (1977) 17.
4. R. Yamada and M. Wake, KEK Internal 81-10 (1982).
5. H. Hirabayashi et al., Jpn. J. Appl. Phys. 20 (1981) 2243.
6. H. Hirabayashi et al., Jpn. J. Appl. Phys. to be published.
7. M. N. Wilson, IEEE Trans Magn MAG-17 (1981) 1815.
8. M. Scherer and P. Turovski, Cryogenics 18 (1978) 515.

Table 3 List of quench characteristics in some cases with $R = 0.05 \Omega$ and with the quench velocities faster than the calculated value using Eq. (4)

Run #	U	L/R	T_{act}	T_{max}	V_{max} (res.)	V_{max} (total)	E_{int}	E_{ext}	$\int I^2(t)dt$
M-13	50. m/sec	58.6 s	27.3 s	62.4	217. v	337. v	14. MJ	15. MJ	$3.07 \times 10^8 A^2sec$
M-14	100. m/sec	58.6 s	27.1 s	61.9	219. v	339. v	14. MJ	15. MJ	$3.05 \times 10^8 A^2sec$
M-15	200. m/sec	58.6 s	26.5 s	60.6	226. v	348. v	15. MJ	15. MJ	$2.98 \times 10^8 A^2sec$

- 14 -

Table 2 List of quench characteristics in the cases that the quench occurs from the edge of coil.

Run #	R	L/R	T_{act}	T_{max}	V_{max} (res.)	V_{max} (total)	E_{int}	E_{ext}	$\int I^2(t)dt$
M- 7	0.005 Ω	586. s	36.7 s	134. K	444. v	458. v	27. MJ	2.7 MJ	$5.34 \times 10^8 A^2sec$
M- 8	0.02 Ω	147. s	38.1 s	119. K	308. v	357. v	19. MJ	9.9 MJ	$4.98 \times 10^8 A^2sec$
M- 9	0.05 Ω	58.6 s	37.9 s	89.6 K	122. v	231. v	8.7 MJ	21. MJ	$4.15 \times 10^8 A^2sec$
M-10	0.1 Ω	29.3 s	27.2 s	56.6 K	28.9 v	450. v	1.9 MJ	27. MJ	$2.76 \times 10^8 A^2sec$
M-11	0.5 Ω	5.9 s	6.0 s	26.7 K	2.1 v	2250. v	0.04 MJ	29. MJ	$0.61 \times 10^8 A^2sec$
M-12	1. Ω	2.9 s	3.0 s	21.3 K	1.0 v	4500. v	0.01 MJ	29. MJ	$0.31 \times 10^8 A^2sec$

- 13 -

Figure Captions

- Fig. 1 One dimensional model introduced to solve the thermal equation.
- Fig. 2 Calculated time variation of temperature distribution after a quench in 1 mφ x 1 m coil. The parameters are as follows; conductor size = 2.0 x 0.359 cm², initial current = 3540 A, current decay time = 58.6 sec, current sharing temperature = 7.1 K, critical temperature at zero current = 8.8 K, initial temperature of the quench = 23 K, eddy current loss = 2.5 x 10⁻⁶ W/cm³ (at t = 0), and time interval in this plot = 0.2 sec.
- Fig. 3 Calculated quench velocities as a function of the axial position from the center in the 1 mφ x 1 m coil for various excitation current.
- Fig. 4 Quench velocities as a function of the solenoid current in the 1 mφ x 1 m coil. Measured data of the quench velocity in the axial direction agree with the simulation result of Eq. (1) with k = 1.6 W/m²·K. Also the transverse velocity calculated from Eq. (5) is shown.
- Fig. 5 Time variation of temperature distribution after a quench in the 3 mφ x 5 m solenoid. A quench back appears at t = 0.46 sec. The parameters are as follows; conductor size = 3.0 x 0.359 cm², initial current = 4500 A, current decay time = 58.6 sec, current sharing temperature = 6.4 K, critical temperature at zero current = 8.6 K, initial temperature of the quench = 20 K, eddy current loss = 5.1 x 10⁻³ W/cm³ (at t = 0), and time interval in this plot = 0.1 sec.
- Fig. 6 Quench velocities as a function of the axial position from the center in the full-size 3 mφ x 5 m solenoid (initial current = 4500 A).

Table 4 List of quench characteristics with R = 0.05 Ω, in the case that the heat capacity of aluminum in conductor is assumed effectively larger due to the bobbin (i.e. C_p(Al) x 1.72). M-20 corresponds to the case with R = 5 mΩ.

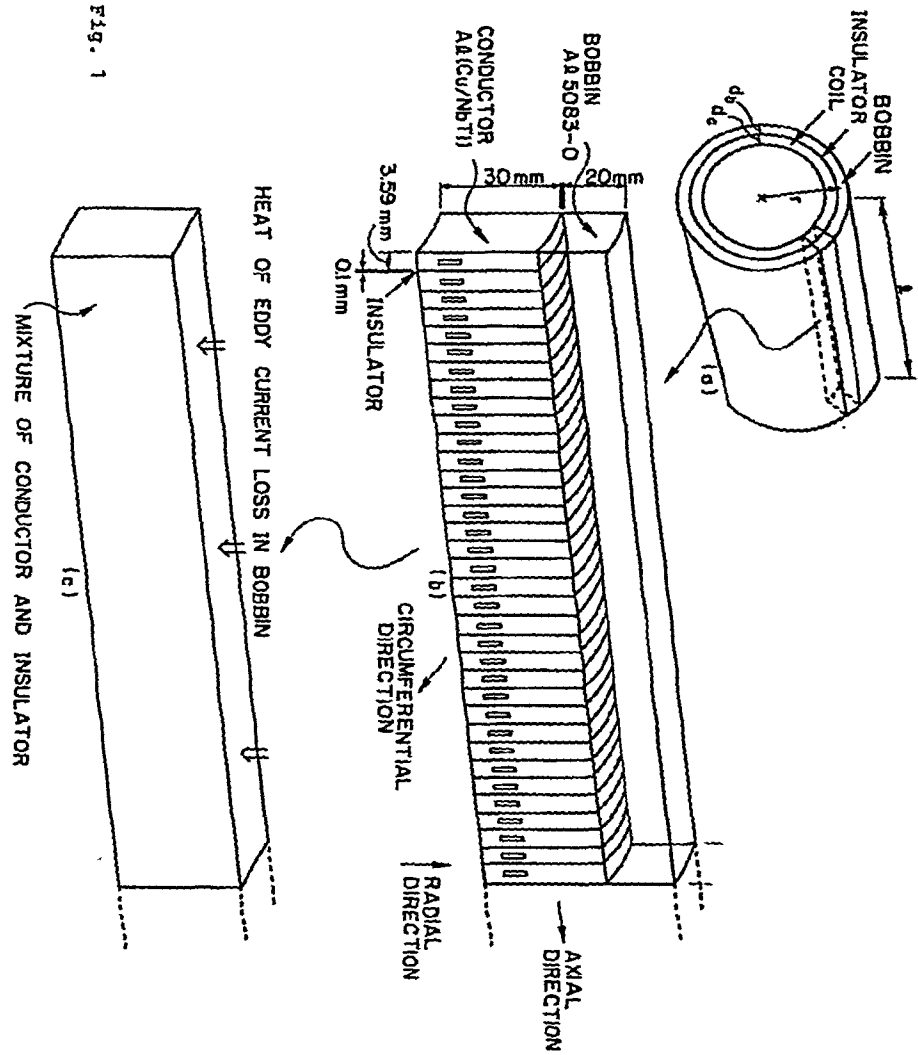
Run #	U ₀	L/R	t _{act}	T _{max}	V _{(res.)^{max}}	V _{(total)^{max}}	E _{int}	E _{ext}	∫i ² (t)dt
M-16	2.8 m/sec	58.6 s	43.2 s	58.2 K	65.2 V	225. V	6.6 MJ	23. MJ	4.57 x 10 ⁸ A ² sec
M-17	50. m/sec	58.6 s	35.4 s	49.9 K	104. V	264. V	11. MJ	19. MJ	3.76 x 10 ⁸ A ² sec
M-18	100. m/sec	58.6 s	34.4 s	49.0 K	111. V	271. V	11. MJ	18. MJ	3.66 x 10 ⁸ A ² sec
M-19	200. m/sec	58.6 s	33.9 s	48.5 K	115. V	275. V	11. MJ	18. MJ	3.61 x 10 ⁸ A ² sec
M-20	200. m/sec	586, s	38.7 s	63.2 K	303. V	316. V	27. MJ	2.5 MJ	4.97 x 10 ⁸ A ² sec

Fig. 7 Resistivity data of aluminum and copper for the program 'QUENCH'.

Percentage of component material is given by volume.

Fig. 8 Heat capacity data of aluminum, copper, titanium and niobium for the program 'QUENCH'.

Fig. 9 An example of the quench behavior of the 3 mφ × 5 m solenoid. The current, the coil resistance, the resistive coil voltage and the maximum temperature in the coil are plotted for the case of M-3 in Table I.



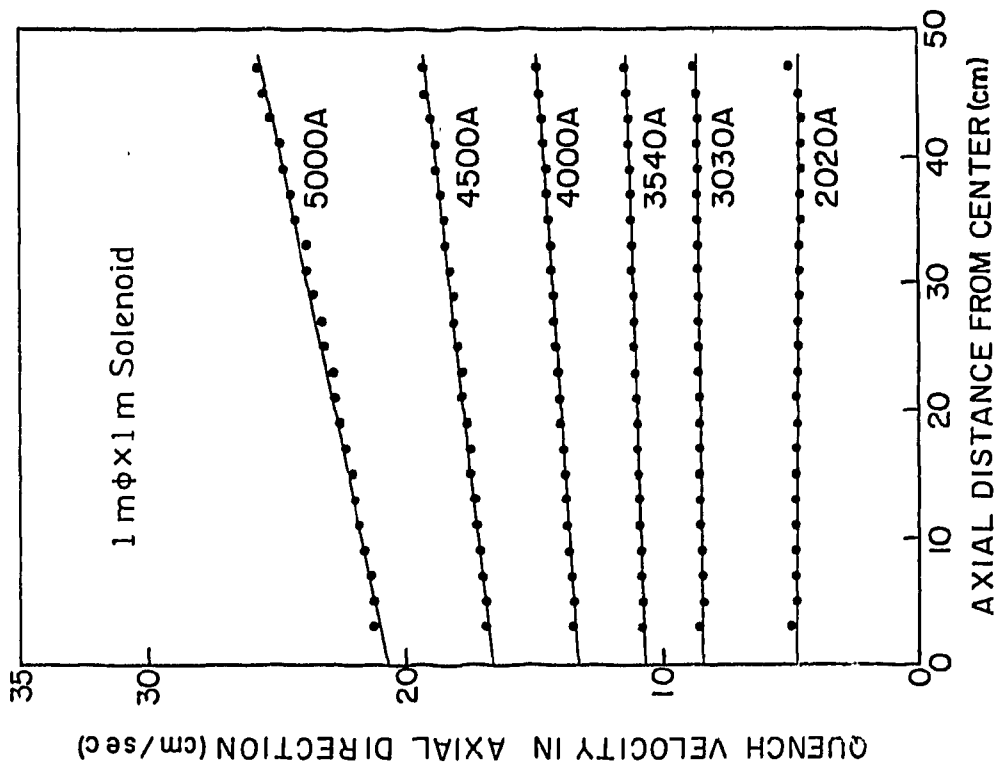


Fig. 3

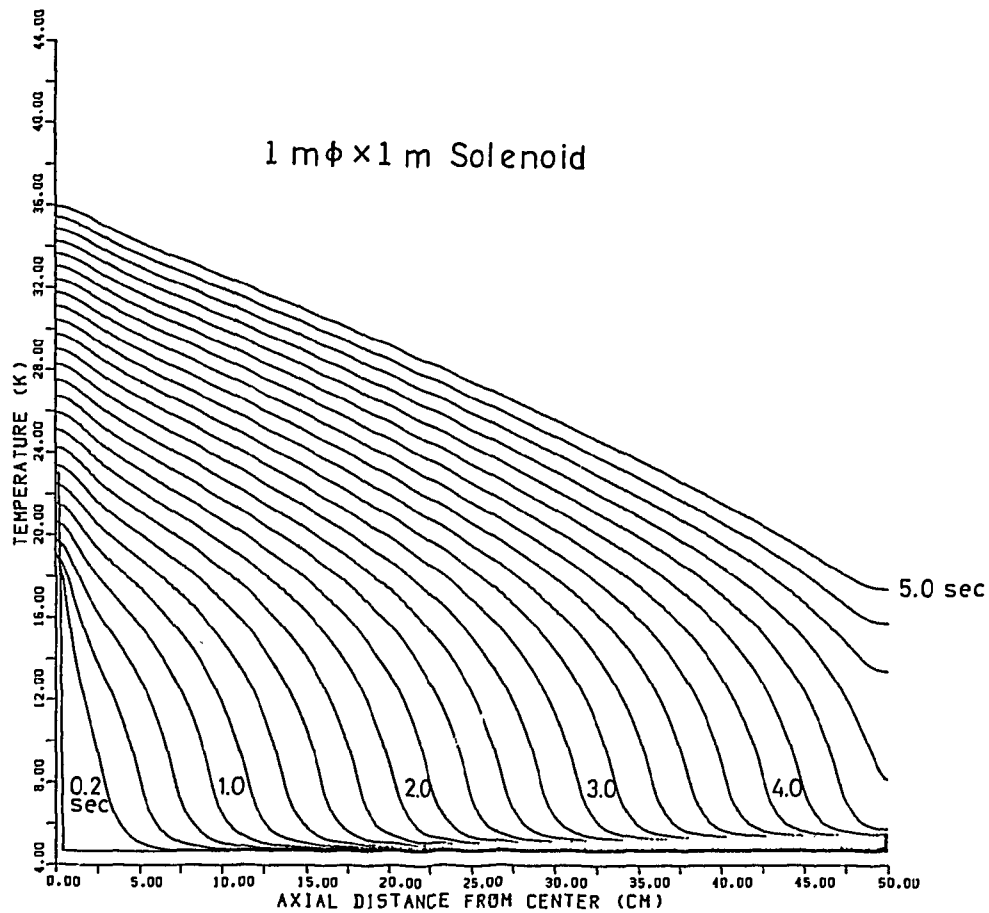


Fig. 2

Fig. 5

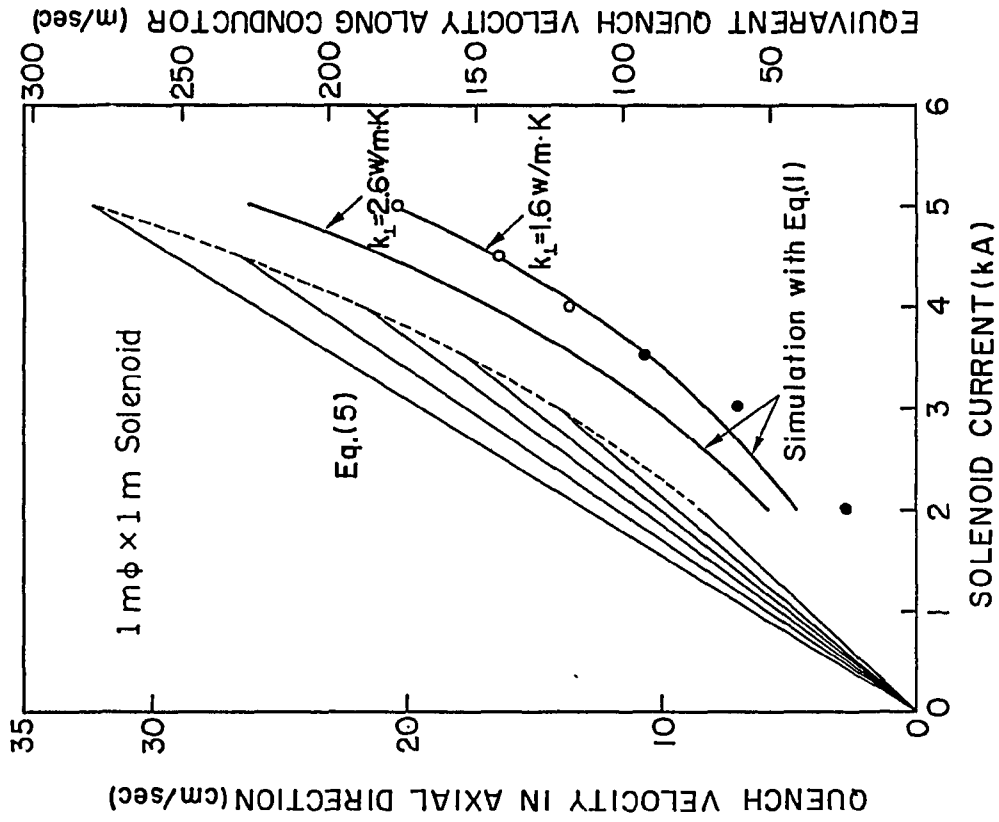
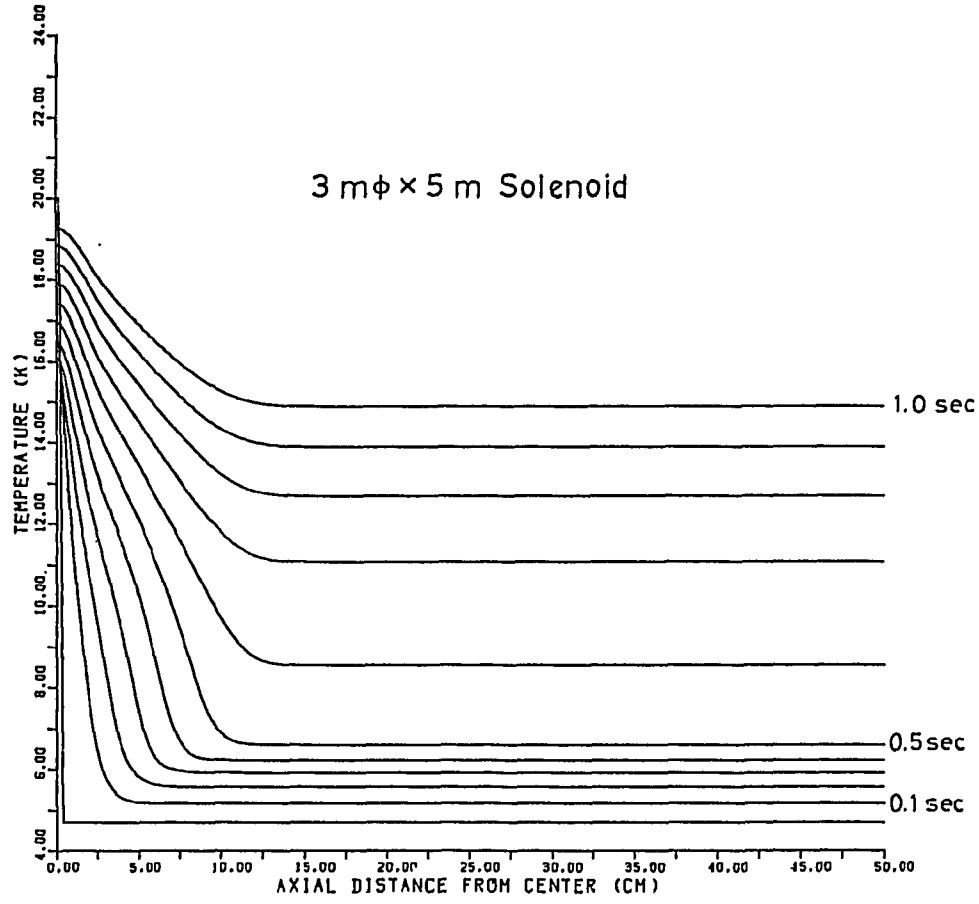


Fig. 4

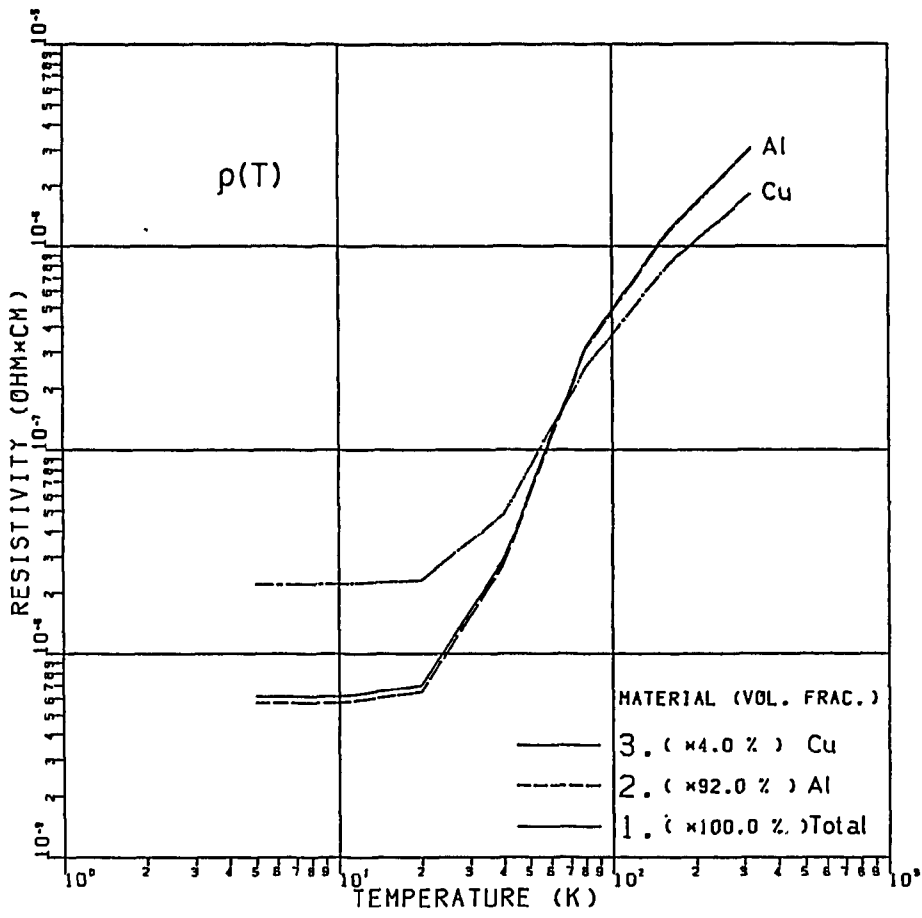


Fig. 7

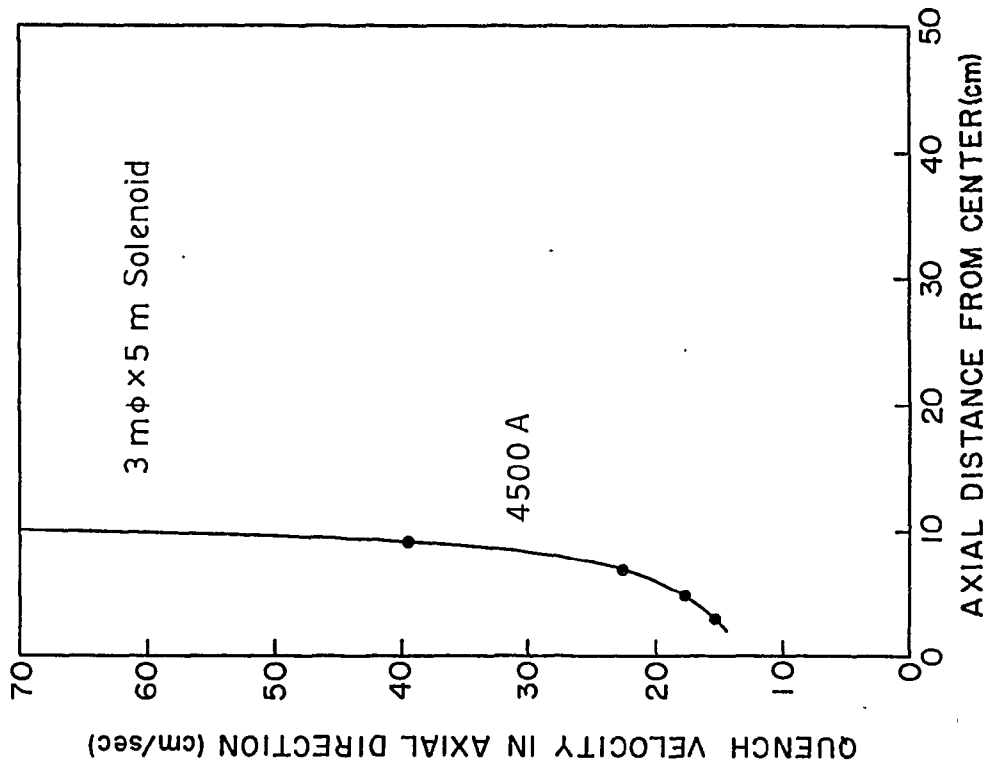


Fig. 6

Run No. M-3

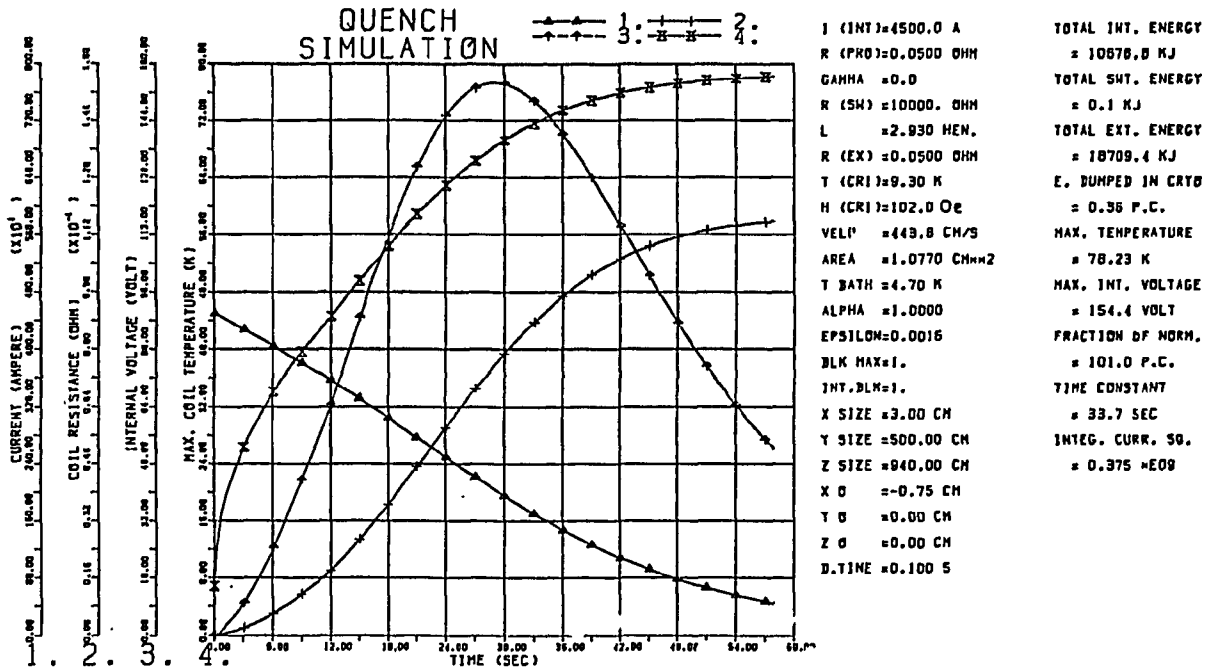


Fig. 9

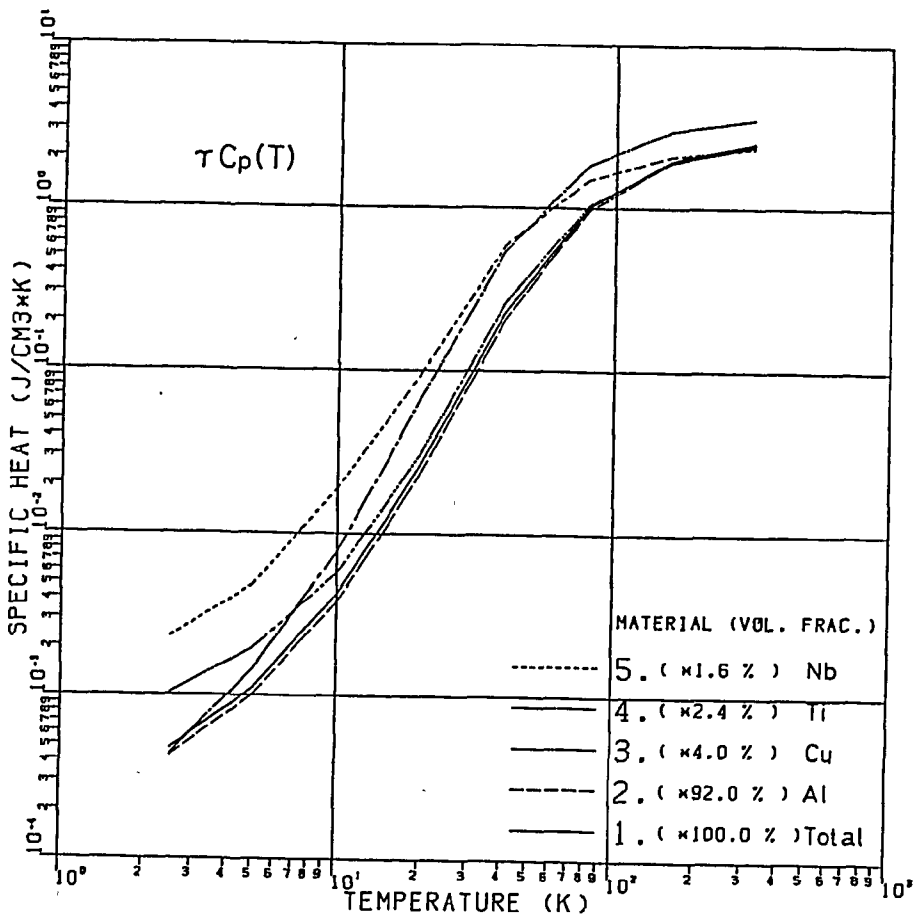


Fig. 8